

Numerical Analysis of Pin Fin Heat Sink with a Single and Multi Air Jet Impingement Condition

N. K. Chougule, G.V. Parishwad, C.M. Sewatkar

Abstract— This study presents the numerical simulation of the 4x4 pin fin heat sink with single jet and 3x3 multi air jet impingement. Thermal performance of both single jet of diameter 15mm and 3x3 array multi air jets of 5mm diameter are evaluated in terms average Nusselt number (Nu_{avg}). Since the total flow area of the nozzle holes for the single jet impingement is the same as that for multi jet impingement, the square root of area is adopted as a characteristic length scale throughout the study. The Reynolds number is varied from 7000 to 11000 at $Z/d=6, 8$ and 10 . It is observed that multijet impingement showed higher heat transfer enhancement than single jet impingement on pin fin heat sink. However with flat plate as target surface single jet impingement showed higher heat transfer enhancement than multi jet impingement for $Re > 7000$ at $Z/d=6$. The results of this paper can help in design of heat sinks with jet impingement, which is commonly used in electronic cooling.

Index Terms— Pin fin, Heat sink, Multi-jet impingement, CFD.

I. INTRODUCTION

In jet impingement technique a thin boundary layer is formed on a heated target surface which results in a higher convective heat transfer coefficient. Many studies on single and multi jet impingement on flat plate have been performed [1-9]. Also works has been carried out for the single jet impingement on the extended surfaces such as pin fin and have reported more enhancement heat transfer [2, 6, and 7]. Recently, several works on the single jet impingement heat transfer from the extended surfaces such as pin fin, pyramid fin, mesh fin, and aluminum foam fin have been implemented and have reported more enhanced heat transfer [1, 2, 6 and 7]. It has been reported that single jet impingement provides gradually decreasing local heat transfer coefficients in downstream regions of single stagnation zone [5] whereas multi jet impingement has a characteristic of multiple stagnation zones which results in the enhancement of heat transfer [4]. However from vast literature survey it is observed that multi air jet impingement on pin fin heat is still challenging.

In this study 4x4 array of 5mm diameter pin fin heat sink with 60mm square base are employed to enhance heat dissipation from a heated target surface in both single jet of 15mm diameter and 3x3 multi air jets of 5mm diameter impingement schemes. The nozzle arrangement as shown in Fig.1. The objective of this study is to compare thermal performance of both single jet and multi air jet impingement on pin fin heat sink in terms average Nusselt number (Nu_{avg}). The influence of Reynold number (Re), the gap between nozzle exit and target surface (Z/d) on the overall heat transfer are examined in detail. As the nozzle diameter is 15 mm for the single jet impingement and 5 mm for the 3x3

multi-jet impingement, the impinging velocity at the nozzle plate and the total area of the nozzle holes are identical both for the single jet and the multi-jet impingements when the airflow rate is the same.

The convective heat transfer coefficient from the heat sinks is calculated from $h=q^*/(T_w-T_0)$, where 'q' is a uniform heat flux from the heater. T_w and T_0 are the averaged surface temperature and the averaged air temperature at the nozzle exits, respectively. Since the total flow area of the nozzle holes for the single jet impingement is the same as that for the multi-jet impingement, the square root of A is adopted as a characteristic length scale throughout this study. Therefore, the averaged Nusselt number (Nu) can be expressed as $Nu_{avg}=(h \sqrt{A})/k$. Where k is the thermal conductivity of air.

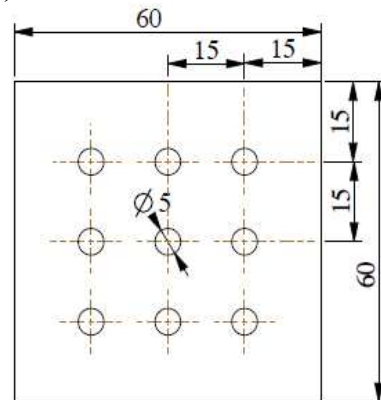


Fig. 1. (a) Multi-jet impingement

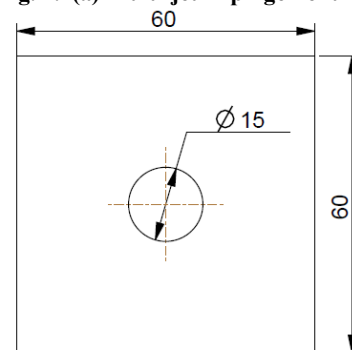


Fig. 1. (b) Single jet impingement

II. MATHEMATICAL MODELING

A. Description of the Physical Problem

The schematic physical model of a multi jet impinging on a Pin Fin Heat Sink (PFHS) which are to be analyzed is shown in Fig. 2. The air jet is discharged through the round nozzle with length l and diameter d is directed normally towards the pin-fin heat sink with base $60 \times 60 \times 6$ mm. subjected to a constant heat flux from below (bottom) and except top

surface all other walls are adiabatic. The jet after impingement will exit from opening with minimum cross flow conditions.

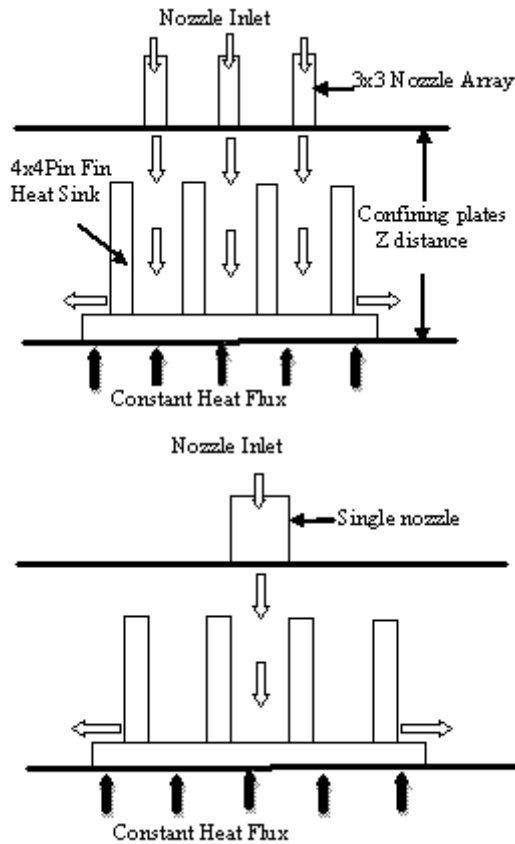


Fig. 2 Schematic 2D diagram of the physical model of single and 3x3 multi-jet 4x4 Pin Fin Heat Sink

The vertical fin array ($n \times n$) consists of a number of fins of height H , diameter D and spacing between two adjacent fin is S , attached to a square base plate of length L and thickness t_b . Nozzle plate consists of $(n-1 \times n-1)$ hole array with same spacing and have same diameter (d) as that of fin diameter. The material of the heat sink is Aluminum. Copper fin gives the best performance, but if the weight and cost of the heat sink is a constraint, then Aluminum fin can be preferable.

B. Geometry and Boundary Conditions

The schematic diagram of the physical geometry domain and boundary conditions of the modeling is shown in Fig.3 As the domain of interest is having rectangular geometry, a Cartesian coordinate system with origin at A. The fin height (H) is taken in z -direction, the longitudinal longest domain in the x -direction (span wise direction), and along the shortest domain in the y -direction (stream wise direction). The computational domain is bounded by the solid domain (heat sink) and fluid domain (Air). The solution domain is filled with stagnant air. It is assumed that the heat is generated inside the heat sink at a uniform rate and can be represented by a constant heat flux from the bottom. If this flux coming out of the heat sink is not dissipated properly, the temperature will go up and it might lead to failure of the electronic devices

on which heat sink is mounted. To cool the heat sink, a finned heat sink is mounted and an air jet is impinging through array of nozzles. The steady jet is exited through array of nozzles and impinged on the heat sink and exit from the openings.

Pressure boundary condition is applied to the faces ABFE, AEHD, DHGC and CGFB (for minimum cross flow condition). At nozzle inlet velocity boundary condition is applied. The faces ABCD and EFGH represent the two confining plates and adiabatic wall condition is applied to them. At the bottom of the heat sink, wall boundary condition is imposed with heat flux $8333W/m^2$ (30 watts for 60×60 base plate). The side walls heat sink is assumed adiabatic thermal boundary condition state. The flow is assumed to be steady, incompressible and three-dimensional. The buoyancy and radiation heat transfer effects are neglected and thermo physical properties of the fluid such as density, specific heat and thermal conductivity are assumed to be constant.

C. Numerical Procedure

The solution domain is filled with stagnant air. The three dimensional Navier-Stokes and energy equations with the standard turbulent model are solved using CFD software (ICEM as mesher and CFX solver) which is combined with continuity and momentum equations to simulate thermal and turbulent flow fields.

As geometry is small enough and we have sufficient computational power so here consider complete geometry for the CFD analyses and created in ANSYS ICEM CFD 12.0. All geometrical dimensions are similar as that of test set up. The opening boundary is sufficiently away from the actual physics so that flow becomes stable and actual flow phenomenon at impinging surface is captured. The structural mesh was created within this domain by using ANSYS ICEM CFD with the option of blocking.

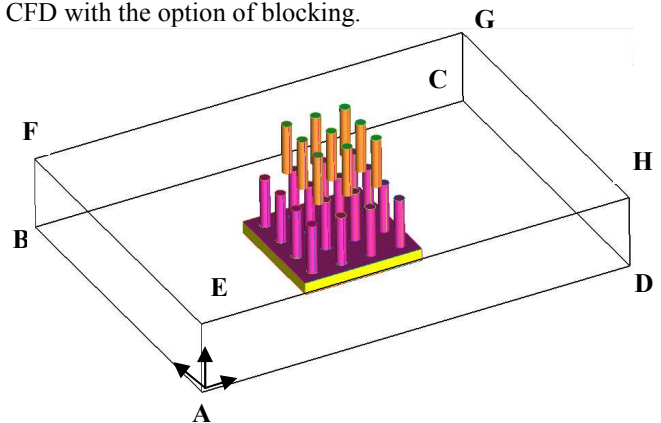


Fig.3 -The computational and Physical domain and Boundary Conditions (BC) of jet impingement

As structured mesh used hence the orthogonally is maintained hence accurate prediction of heat transfer characteristics there. As hexa mesh used over the entire computational domain hence no need to use the prism mesh at the near wall region to predict the near wall flow phenomenon. Hence to capture the near wall flow phenomenon dense the hexa mesh at near wall region by means of using the linear mesh law algorithm and then bunching the all parallel edges as shown in Fig. 4. This was

not only capture the near wall flow phenomenon but also increases the smoothness of the mesh. Dense mesh also helps to control the y^+ . Grid independency on heat transfer characteristics was checked by changing the element size from 0.15 million to 1.1 million which follows that about 0.72 million was good enough for present analysis from view point of accuracy and computational time.

The numerical simulations were carried out using the commercial CFD solver ANSYS CFX version 12.0. The flow and turbulent fields have to be accurately solved to obtain reasonable heat transfer predictions. Higher resolution scheme is used for all terms that affect heat transfer. Higher order discretization scheme is used for the pressure; momentum, turbulent kinetic energy, specific dissipation rate, and the energy. Flow, turbulence, and energy equations have been solved. In the fluid domain the inlet boundary condition is specified the measured velocity and static temperature (300K) of the flow were specified at the inlet of the nozzle. No-slip condition was applied to the wall surface. In fluid domain there is also opening boundary condition in which flow regime is subsonic, relative pressure is 0 Pa with the details of operating temperature (300 K) and the turbulence intensity of 5%. In solid domain the constant heat flux (8333W/m²) was given with the initial temperature condition automatic with 40oC at the base of heat sink and the sides of heat sink base plat are adiabatic.

To simplify the solution, the variation of thermal and physical properties of air with temperature is neglected. The flow field was numerically examined by use of CFX (ANSYS), assuming the steady-state flow. The overview of the meshed Computational domain is shown in Fig.4.

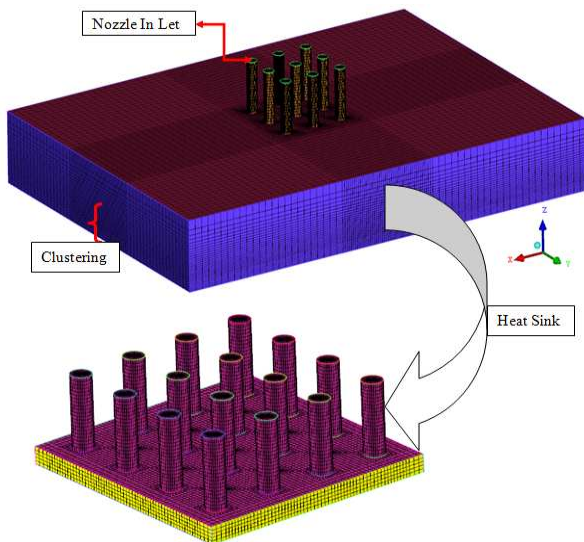


Fig. 4 Computational domain of jet impingement on pin fin heat sink

D. Near-Wall Treatment

Numerical models of turbulence near the wall, commonly tackled by two approaches. In the first obvious approach, the grid near the wall is constructed at sufficiently high resolution to properly resolve flow in the entire viscous sub layer and turbulent boundary layer with turbulence equations

intended for use at low cell Reynolds numbers. This requires a model capable of resolving turbulent behaviors very close to the wall, and a large computation effort. The alternate method uses algebraic equations to relate steady and fluctuating velocity and scalar profiles to wall distance and surrounding fluid properties. These wall functions predict the flow properties in and above the viscous sub layer. This method requires only a single cell in the sub layer, and thus requires less computational time. Relations for high Re parallel flows such as the “law of the wall” are based upon flows in different geometry than that of the impinging jet and may not produce a correct velocity profile near the wall, especially in cases where the flow separates or reverses on the target surface. The standard law of the wall is based upon the absence of pressure gradients near or along the wall, clearly a different flow field than that seen in the stagnation region of an impinging jet. The non equilibrium law of the wall is based upon differing turbulent energy generation and destruction rates and accounts for pressure gradients.

Specific difficulties arise with the numerical modeling of impinging jets. A number of models reviewed below, such as k- ϵ , have been optimized for free-shear flows such as submerged jets. Some models, such as k- ω , perform best in boundary-layer flows such as the wall-jet region. Unfortunately, the impinging jet problem contains both of these as well as significant pressure gradients in the stagnation region. The normal strain and the rise in fluid pressure in the stagnation region affect the turbulent flow through distinct terms in the second-moment RANS equations. The pressure plays a part in the turbulent diffusion term.

The effects of changing pressure play an even greater role in the pressure-strain rate correlation term. Unlike the turbulent diffusion term, which most models focus on approximating, the pressure-strain correlation was usually of secondary interest. As a result, most models have simpler and less accurate predictions for turbulent effects in the stagnation region. A wide variety of equation sets have been implemented to model these pressure-strain rate correlation terms related to $\nabla u'$ and ∇u with varying success. The two equation eddy-viscosity models, such as k- ϵ , contract the rank-2 tensors in the equations to eliminate terms, and thus drop these terms. That is, the two-equation models are based around assumptions about the low importance of pressure gradients and the minimal anisotropy of the Reynolds stresses, and experiments have shown that these modeling assumptions do not apply in the stagnation region.

III. RESULTS AND DISCUSSIONS

A. Effect of Re on Local Temperature Distribution

On this evaluation line temperature plot as a function of X at Z/d = 8 for Single & Multi-jet on 4x4 Pin Fin Heat Sink for Re=7000, 9000 and 11000 is shown in Fig. 5

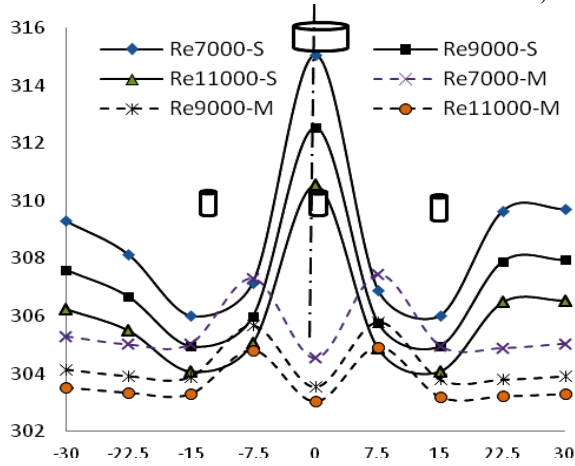


Fig.5. Typical temperature plot as a function of X at Z/d = 8 for Single & Multi-jet on 4x4 Pin Fin Heat Sink

It is observed that as we increase Re, target surface become cooler. In all cases of multi-jet impingement it is also observed that area below nozzles has lowest temperature compared to other area of target surface. Compared to single jet impingement, in multi-jet impingement, more uniform temperature distribution and lower temperature is observed at all the ranges of Re and Z/d ratio.

B. Effect of Re and Z/d on Temperature Distribution

Temperature contours on the middle cross section of the heat sink for single jet impingement on 4x4 pin fin heat sink at different Re and Z/d are shown in Fig. 6 and 7 respectively.

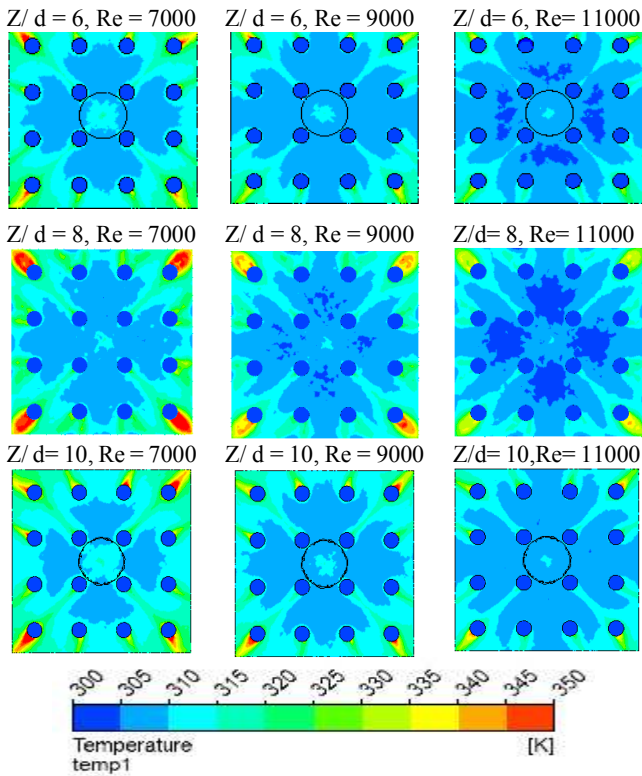


Fig. 6. Temperature contours for single jet impingement on 4x4 Pin Fin heat sink

Z/d = 6, Re= 7000 Z/d = 6, Re= 9000 Z/d= 6, Re= 11000

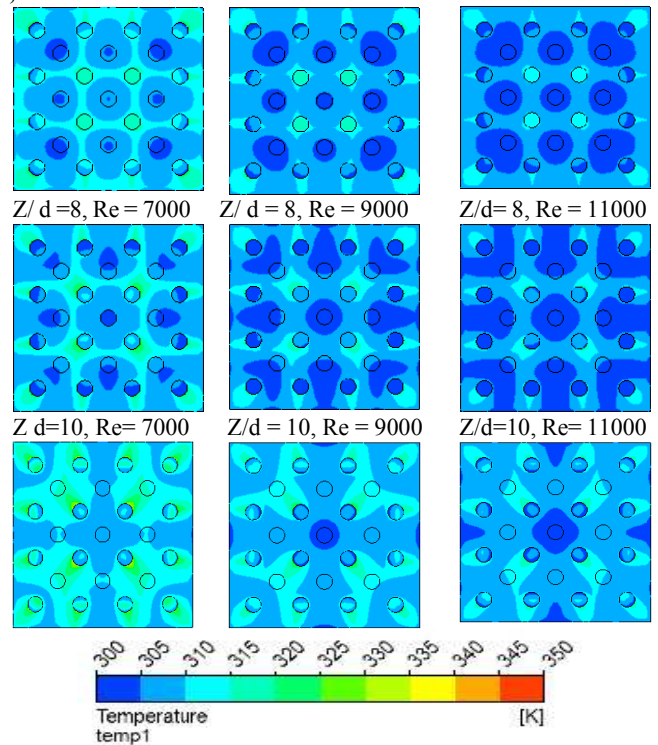


Fig. 7. Temperature contours for multi jet impingement on 4x4 Pin Fin heat sink

These temperature contour plots show that for higher Reynolds number, average temperature of heat sink is lower due to localized cooling and in case of multi-jet, there is uniform distribution of temperature compared to single jet case. It is also observed that the portions of plate below nozzle area are cooled intensively than other area. For the multi-jet case, as shown in Fig. 7, the peak in heat transfer was located directly on the jet centerline for middle nozzles, where the cross flow is still small. However for outer nozzles as the cross flow developed, the peak position is observed to shift slightly downstream as the increased cross flow displaced the jets. Figure 8 shows the distribution of average temperature on heat sink at different Z/d and Re for both single and multi jet case. In case of single jet, temperature drop linearly as we increase gap between nozzle exit and heat sink, whereas in multi jet case it is observed that average temperature is minimum at Z/d =8. The variation range of temperature distribution is lower in multi jet impingement which is desirable in most of the engineering applications.

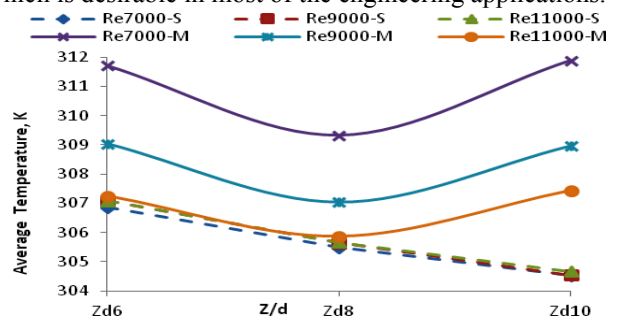


Fig. 8. Average Temperature plot against Z/d for single jet impingement on 4x4 Pin Fin heat sink

C. Effect of Re and Z/d on local and average Nusselt number

Fig.9 shows CFD local Nu for Re=7 000, 9 000 and 11 000 at Z/d = 8 for both single and multi-jet impingement on 4x4 pin fin heat sink.

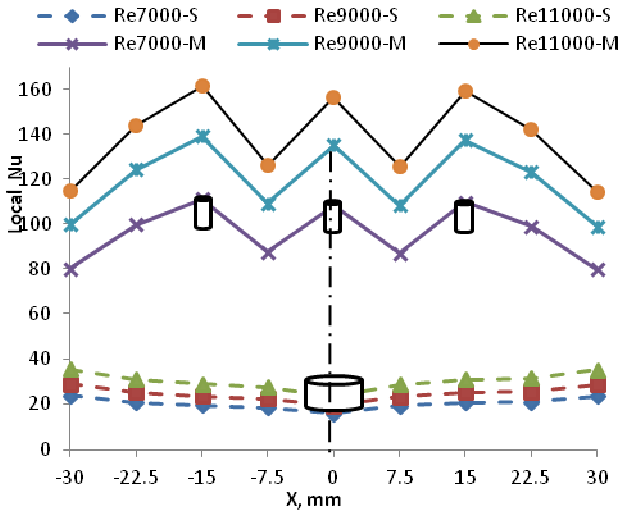


Fig. 9 Typical Nusselt number plot as a function of X at Z/d = 8 for Single & Multi-jet on 4x4 Pin Fin Heat Sink

The local Nu is measured on the central line of target surface. Nu distribution of multi-jet impingement is higher as compared to single jet, due to multi stagnation points. For all the other Z/d cases, the Nusselt number is maximum on the stagnation point and decreases monotonically from the stagnation and for higher Re, Nu is maximum. The effect of Z/d on the stagnation point Nuavg is plotted in Fig. 10. The nozzle plate-to-heated surface separation distance (Z/d) also significantly affects thermal transport due to adjacent jet interference (A. M. Huber (1994), J. Y. San (2001)). Nuavg reaches maximum at about Z/d equal to 6. It is also found that the length of potential core is about 5 times the jet nozzle diameter. Beyond the potential core, with further increase in axial distance, the interaction between the attenuation of approaching jet velocity and the continuous increase in centerline turbulence intensity brings about a maximum heat transfer coefficient at Z/d = 6.

As the Z/d ratio increases from 6 to 10, the mean heat transfer coefficient drops in both single and multi-jet impingement cases. Further increase of causes the flow to behave as the unconfined jet impingement. However the change of the mean heat transfer coefficient in the multi jet case is about four times that of single jet case due to multi stagnation points. As Z/d changes from low level (6) to high level (10), havg decreases from 43.23 W/m² K to 30.21 W/m² K and from 185.63 to 151.315 W/m² K in single and multi-jet cases respectively at Re11000. Thus the average heat transfer coefficient decreases by 30.1% in single jet impingement and 16.4% in multi-jet impingement. This indicates that as the nozzle is moved farther away from the target surface, rate of the heat transfer decrease in single jet case is more than multi-jet case. In another word, at constant

Re, as Z/d increases, Nuavg gradually decreases due to reduced momentum of free jet beyond the separation distances.

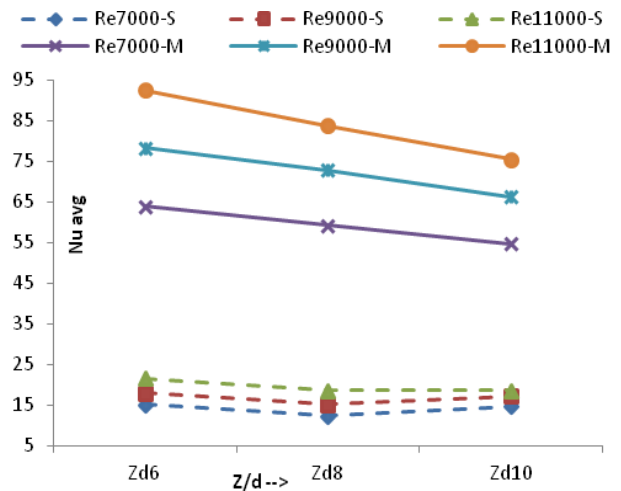


Fig. 10. Average Nusselt number plot as a function of Z/d

D. Effect of Re and Z/d on average heat transfer coefficient

The effect of Z/d on the average heat transfer coefficient is plotted in Fig. 11. As Re increases from low value (7000) to high value (11000) at Z/d=6, the mean heat transfer coefficient increases from 30.34 W/m²K to 43.23 W/m²K and from 128.183 W/m²K to 185.63 W/m²K in single and multi-jet cases respectively. Thus in case of single jet the Re increases about 57%, the heat transfer increases 42% and in multi-jet case the Re increases about 57%, the heat transfer increases 45%. This means that the heat transfer coefficient depends strongly on the air velocity. In terms of dimensionless groups, it means that Nuavg is strongly affected by Re since the air velocity occurs only in Re. Thus the heat transfer rate higher due to promoted turbulence.

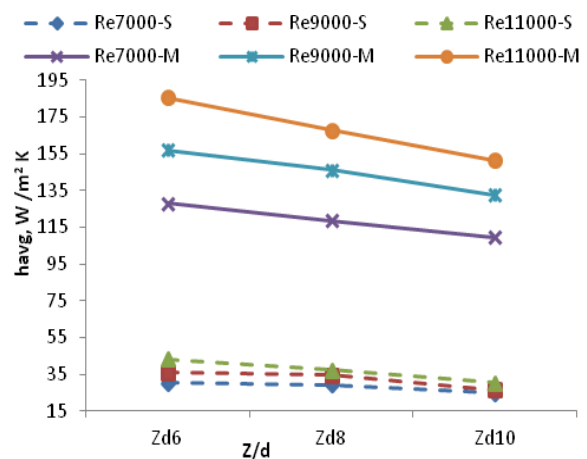


Fig. 11 Average heat transfer coefficient plot as a function of Z/d

E. Velocity contours for single and multi jet impingement

Figure 12a and 12b shows velocity contours for both single and multi-jet cases at $Z/d = 6$ to 10 and $Re = 11000$ respectively. The air after impinging on the stagnation zone starts to accelerate towards exits. Single jet impingement has only one stagnation point compared to multi-jet impingement; therefore the thermal performance of multi-jet configuration is better than single jet case. Also it is observed that most of the fins are not exposed to impinging air in case of single jet impingement.

For the multi-jet case, the central jet is not disturbed at all Z/d ratio and the jet is impinged directly below nozzle as the cross flow is still small at this location. However for $Z/d > 6$ the outer jets spread more and tries to divert outside due to strong development of the cross flow which affects heat transfer rate. As we increase Z/d , the jet-to-jet spacing should also increase otherwise jet may mix before impingement and substantially affects the velocity distribution and heat transfer rate. In case of higher Z/d ratio there is a higher momentum exchange between impinging fluid and quiescent fluid due to this the jet diameter becomes broader and spreads over more surface area. In case of low Z/d ratio the same amount of fluid spreads over lesser surface area causing a higher heat transfer rate.

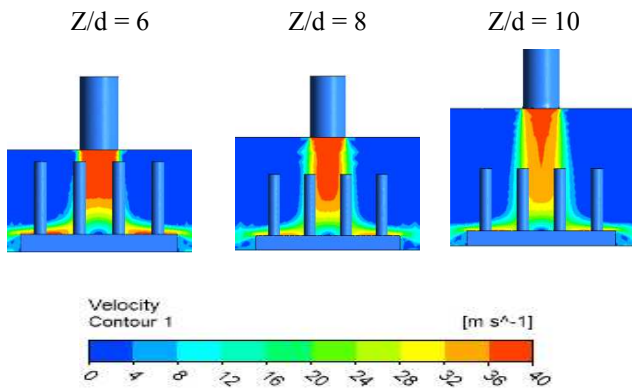


Fig. 12 a. Velocity contours for single cases at $Z/d = 6$ to 10 and $Re = 11000$

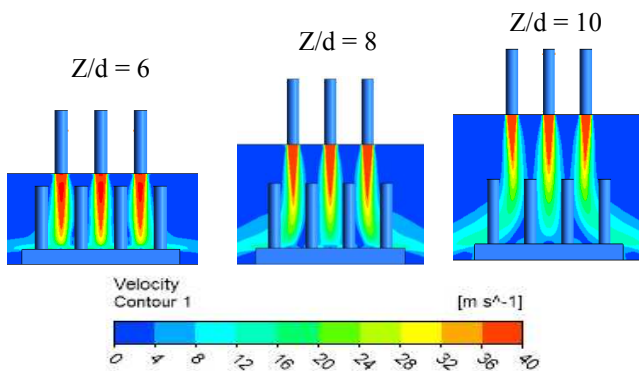


Fig. 12 b. Velocity contours for multi-jet cases at $Z/d = 6$ to 10 and $Re = 11000$.

F. Comparison of Computational and Experimental Results

The objective of this section is to experimentally confirm the numerical results.

Table I. comparison between experimental and CFD results

Z/d	Re	EXPERIMENTAL RESULTS h, W/, m ² k	CFD RESULTS h, W/, m ² k	% error
6	7000	167.0	175.8	5.0
6	9000	195.5	205.9	5.0
6	11000	229.1	242.9	5.6
8	7000	152.6	167.4	8.8
8	9000	190.9	206.2	7.4
8	11000	210.5	228.4	7.8
10	7000	130.2	137.3	5.1
10	9000	165.6	176.7	6.2
10	11000	181.1	194.7	6.9

To simulate the above experimental conditions in context of numerical analysis, the same geometry, boundary conditions are applied and also temperature monitoring points are located at the same position where thermocouples are physically located. Table I shows the comparison between experimental and numerical results for $z/d = 6$ to 10 and $re = 7000$ to 11000 . For the range of parameters considered in this investigation a fair agreement between numerical and experimental results is observed ($\pm 5\%$ error).

IV. CONCLUSION

The present work investigated heat transfer and fluid flow characteristics within an impingement model of single and multi jets at different Reynolds numbers and Z/d ratio. The multi-jet impingement shows 3-4 times higher cooling performance compared to single jet due to high saturated convection heat transfer coefficient in the core region of the jet and multi stagnation points. Compared to single jet impingement, in multi-jet impingement, more uniform temperature distribution and lower temperature is observed at all the ranges of Re and Z/d ratio. Also the variation range of temperature distribution is lower in multi jet impingement which is desirable in most of the engineering applications.

As the Z/d ratio increases from 6 to 10 , the mean heat transfer coefficient drops in both single and multi-jet impingement cases. Further increase of causes the flow to behave as the unconfined jet impingement. The highest overall heat transfer coefficients with both single and multi-jet configurations is achieved at $Z/d = 6$. As we increase Z/d , the jet-to-jet spacing should also increase otherwise jet may mix before impingement and substantially affects the velocity distribution and heat transfer rate.

REFERENCES

[1] H. A. El-Sheikh and S. V. Garimella, "Heat transfer from pin-fin heat sinks under multiple impinging jets," IEEE Trans. Adv. Packag., vol. 23, no. 1, pp. 113-120, Feb. 2000.

[2] Y.T. Yang, H.S. peng, "Numerical study of pin fin heat sink with un-uniform fin height design", International Journal of heat and mass transfer, vol. 51 pp. 4788-4796, 2008 .

- [3] L. G. Hansen and B. W. Webb, "Air jet impingement heat transfer from modified surface," Int. J. Heat Mass Transfer, vol. 36, pp. 989-997, 1993.
- [4] N.K. Chougule, G.V.Parishwad, P.R.Gore, S Pagnis, "CFD Analysis of Multi-jet Air Impingement on Flat Plate," The World Congress on Engineering 2011.
- [5] H. Martin, "Heat and mass transfer between impinging gas jet and solid surface," Adv. Heat Transfer, vol. 13, pp. 1-60, 1977.
- [6] A. Hani, El-sheikh and Suresh V. Garimella, "Enhancement of air jet impingement heat transfer using pin fin heat sinks", IEEE transactions on components and packaging technology, vol.23, no.2, 2000.
- [7] H.H. Jung and J.G. Maveety, "Pin fin heat sink modeling and characterization", 16th IEEE semi-therm symposium, 0-7803-5916-x, 2000.
- [8] S. Young Kim, M.Ho Lee, and Kwan-soo Lee, "Heat removal by aluminum-foam heat sinks in a multi-air jet impingement", IEEE transactions on components and packaging technologies, vol. 28, no. 1, pp. 142-148 march 2005.



Prof. C. M. Sewatkar is presently working as Assistant Professor in Department of Mechanical Engineering, Government College of Engineering, Pune. Place of Birth: Yavatmal, Date of Birth: 17th September 1970.

NOMENCLATURE

- Nu_{avg} Average Nusselt number
- d Nozzle diameter, m
- Z Distance between nozzle exit and impinging plate, m
- Z/d Dimensionless jet to target plate spacing
- V Mean velocity at jet exit, m/s
- Re Reynolds number based on jet exit diameter
- $= \frac{\rho V d}{\mu}$

AUTHOR BIGRAPHY



Prof. N.K. Chougule is presently working as Assistant Professor in Department of Mechanical Engineering, Government College of Engineering, Pune. Place of Birth: Kurundwad, Date of Birth: 08th July 1968. His major areas of interest are Numerical modeling, CAD/CAM/CAE. Mr.N.K. Chougule is

life member of Indian Society for Technical Education (ISTE), New Delhi (India). Currently he is pursuing Ph.D. under the guidance of Dr. G.V. Parishwad.



Dr. G.V. Parishwad is presently working as a Professor in the Department of Mechanical Engineering, College of Engineering, Pune. Place of Birth: Belgaum, Date of Birth: 25th March 1960. Educational Qualification: Ph.D. (Thermal Engineering) from Motilal Nehru National Institute of Technology, Allahabad (India) year of passing 1998. Prof. Parishwad is having more than 4

years of Industrial and 23 years of teaching experience. His major field of interest is Thermal Engineering and Renewable Energy. Dr. Parishwad has published 11 research papers in international journal, 4 in national journal, 27 papers in International conferences and 33 in National Conferences. 2 students have completed their Ph.D. 2 more have submitted their Ph.D. Thesis and 5 students are pursuing their Ph.D. under the guidance of Prof. Parishwad. He has visited China, Bangkok, Malaysia, Germany, Netherlands, Austria, etc. for academic purpose. He is Life Member of many Professional Bodies such as Fellow of Institute of Engineers, Indian Society of Technical Education, Indian Society of Mechanical Engineers, Solar Energy Society of India, etc. At present he is the **Chief Coordinator** of the Institute for **Technical Education Quality Improvement Program, (TEQIP) Phase-2** under which the institute has received the Funding of Rs. 125 Million from World Bank for the development of its PG infrastructure and Research at the Institute.